Journal of Sciences, Islamic Republic of Iran 32(2): 143 - 157 (2021) http://jsciences.ut.ac.ir
University of Tehran, ISSN 1016-1104

Investigation of Petrological Characteristics of The Upper Mantle in Hadji-Abad Ophiolitic Complex (South of Iran): Based on Mineral Chemistry

M. Soltani Nezhad[1], H. Ahmadipour[1*], A. Moradian[1], A. Zahedi[2], K. Nakashima[3]

[1] *Department of Geology, Faculty of sciences, Shahid Bahonar university of Kerman, Kerman, Islamic Republic of Iran*
[2] *Department of Geology, College of Sciences, University of Sistan and Baluchestan, Zahedan, Islamic Republic of Iran*
[3] *Department of Earth and Environmental Sciences, Yamagata University, Yamagata, Japan*

Received: 8 June 2020 / Revised: 15 September 2020 / Accepted: 16 October 2020

Abstract

The mantle peridotites of the Hadji-Abad ultramafic complex in Hormozgan province, show some petrological evolutions of the upper mantle of southern Iran. The complex includes harzburgite, lherzolite, dunite and chromitite. Evidences such as different generations of minerals, lobate boundaries between grains, elongation of cr-spinels and pyroxenes, incongruent melting related textures and exsolution lamellae of clinopyroxene in orthopyroxene show that the rocks in this peridotites have past a complex petrological history. The chemical composition of chromites in the Hadji Abad dunites and chromitites is similar to that of boninite melts, while, the mineral chemistry of the harzburgitic and lherzolitic show that the host peridotites belong to the upper mantle and have been depleted from incompatible elements due to 15 to 20 percent partial melting. Geo-thermometric calculations reveal that the studied peridotites equilibriated in upper mantle and spinel-peridotite stability field. Using tectonomagmatic discrimination diagrams shows that the Hadji-Abad ultramafic complex is part of an oceanic lithosphere above suprasubduction zone which has undegone partial melting, high temperature deformations and mantle metasomatism processes associated with this environment. These evidences along with the geological and tectonic setting of the Hadji Abad complex adjacent to the Zagros thrust indicate that the complex probably was created in a suprasubduction zone oceanic mantle section and then tectonically emplaced as part of Esfandagheh-Hadji-Abad mélange in the current situation during the upper Cretaceous. This information confirm the dependence of the Esfandagheh-Hadji-Abad ophiolite mélange on the Neotethyan oceanic lithosphere in southern Iran.

Keywords: Ophiolite; Chromitite; Suprasubduction zone; Hadji-Abad, Iran.

Introduction

Various studies show that ophiolite complexes form in different geo-tectonic settings [1]. Mineralogical and petrological data of upper mantle peridotites in these complexes are of particular importance to evaluate processes affecting their formation and determining the geo-tectonic setting of ophiolite complexes [2, 3, 4].

* Corresponding author: Tel: +989133430397; Fax: +983431322222; Email: hahmadi@uk.ac.ir

Besides, different studies demonstrated that the formation of chromite deposits and related ultramafics are strongly controlled by tectonic setting [5]. Recently, several petrological investigations of ophiolitic complexes (Sikhoran, Soghan, Abdasht, Dehshikh) on the South-eastern Zagros ophiolites and associated Esfandagheh-Hadji-Abad coloured mélange which is also included in this study have been done and show that they belong to the suprasubduction zone setting [6, 7, 8, 9, 10], however, no detailed petrological study has been performed on the Hadji-Abad complex. So, in the present work, we have studied this complex in order to complement petrological studies on Esfandagheh-Hadji-Abad coloured mélange ultramafic complexes. The aims of this paper are, 1) description of field and petrographical characteristics of the Hadji-Abad peridotites. 2) presentation of chemical characteristics of minerals and the host rocks and 3) using these tools for understanding petrological evolutions of the complex.

Materials and Methods

Although systematic sampling of ultramafic units was difficult due to the effect of tectonic phases in the region and advanced alterations affecting these rocks, but attempts were done to select the appropriate samples of peridotitic rock types with the least alteration effects and close genetic linkages. After preparing microscopic thin sections and performing petrographic studies, in order to determine the chemical composition of minerals and to calculate their structural formula, several polish-thin sections from the Hadji-Abad harzburgites, lherzolites, dunites and chromitites prepared and then, 227 point analyses were performed on olivine, orthopyroxene, clinopyroxene and chromium spinels of the studied rocks. The sample names and their locations are shown in the Figure 1. The JEOL-JXA-8600M electron microprobe analyzer with 15–KV accelerator voltage and 2×10^{-8} Amp rays was used in the Department of Earth and Environmental Sciences at the University of Yamagata, Japan for analytical purposes. Then, the construction formula of minerals was calculated by using the obtained results. According to the results of microprocessor-based and oxygen-based analyses, the ideal minerals formula was obtained by specialized software. Despite the fact that ultramafic rock samples of the region were depleted of incompatible elements, the amount of these elements in rocks is mostly lower than the detection limit of the device.

Results

Geological setting

Iranian ophiolitic complexes comprise parts of the Middle East ophiolite belt that is connected to the other Asian ophiolites, such as Pakistan in the east, and Mediterranean ophiolites, including those located in Turkey, Greece and eastern Europe in the west [11]. The Hadji Abad complex is a part of Zagros thrust

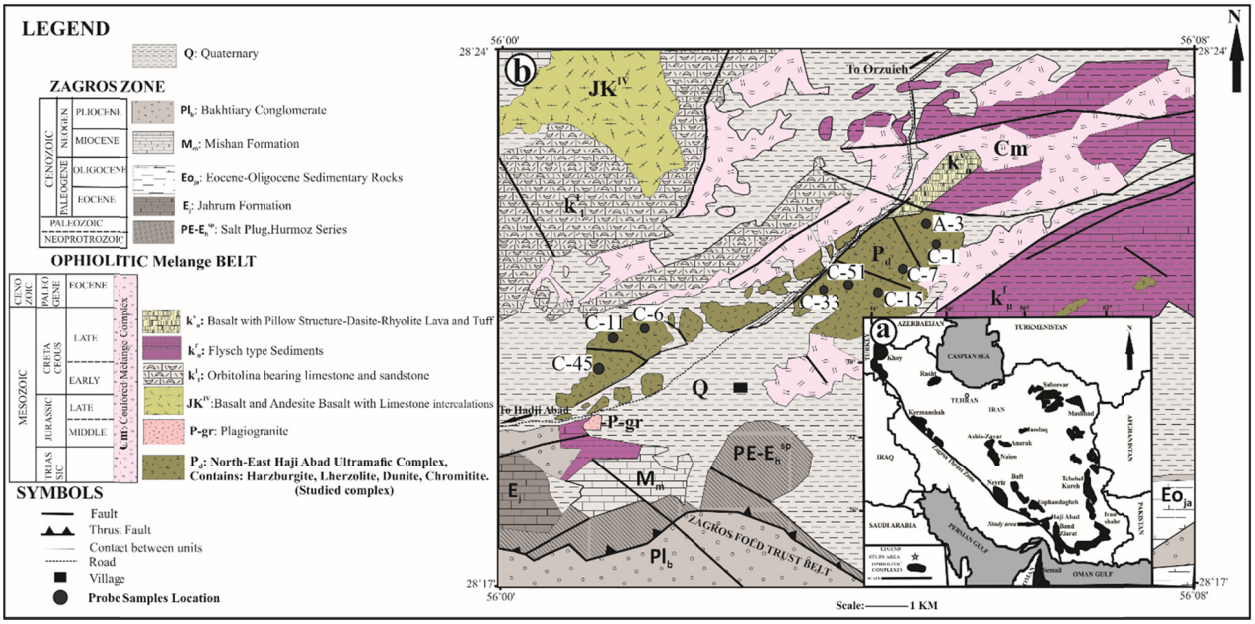

Figure 1. (a) Position of the Hadji-Abad ultramafic complex among other Iranian ophiolites. (b) Geological map of Hadji-Abad region adapted from the map of the 1: 100000 Orzueiyeh [16].

ophiolite belt and is located at the northern edge of the Zagros thrust adjacent to the south-eastern part of the Sanandaj-Sirjan zone (south of Iran). In this area, several ophiolitic complexes such as Abdasht, Soghan, Deh Sheikh and Sheikh Ali form an ophiolitic belt called Esfandagheh-Hadji Abad coloured melange belt [12]. The Zagros thrust ophiolite belt itself forms the central part of the Tethyan ophiolite belt with a length of more than 3000 km, extending from Cyprus to Oman. It connects the alpine ophiolites to the Himalayas [13]. According to McCall, [14], this area is part of the southern margin of the Sanandaj-Sirjan/ Bajgan-Durkan section, separated from the Neyriz Ophiolites(Fig. 1. a). Shahabpour [15] regards this ophiolitic melange as a part of the Neyriz ophiolitic melange which is located on the south-east edge of the Zagros thrust zone.

The Hadji-Abad Ultramafic Complex covers an approximate area of 8 km^2 as a massive block with a northeast-southwest extension and forms part of the Esfandagheh-Hadji-Abad ophiolitic melange with the Triassic age [16]. The studied area has an imbricated structure in which the thrust faults are totally extended from the northeast and north to southwest and south. In the studied area, there are different rock units. In the south and southwestern part, salt Hormoz Formation (Precambrian-Cambrian), Jahrom Formation dolomitic limestones (Mid-Eocene), fossilized limestone-marl layers of Mishan Formation (Lower-Middle Miocene) and Bakhtiari conglomerate (Pliocene) occur. As illustrated in Figure 1, the major parts of the study area covered by ophiolitic units. Triassic ultramafics which are investigated in the present work, occur in the central parts, small outcrops of middle Jurassic plagiogranites are located in the east, basalts and basaltic-andesite lava flows along with the limestones are found in the north-west, the Cretaceous orbitolina bearing limestones and sandstones occur in the northwest, fleysch type sediments in the northeast and the Upper Cretaceous acidic volcanic rocks are seen in the north. Besides, there are some outcrops of Lower Cretaceous undivided coloured melange parts (CM) in the cental and northern parts of the area [16], (Fig. 1. b).

The lithological units and Field relations

In general, in the Hadji-Abad region, ophiolitic rocks include mantle and crustal units. In the mantle part, a variety of ultramafic rocks (such as dunite, harzburgites and lherzolites) could be found; while in the crustal part, pillow lavas, pelagic limestone and a small portion of acidic volcanic rocks occur (Fig. 2. a). Since this paper

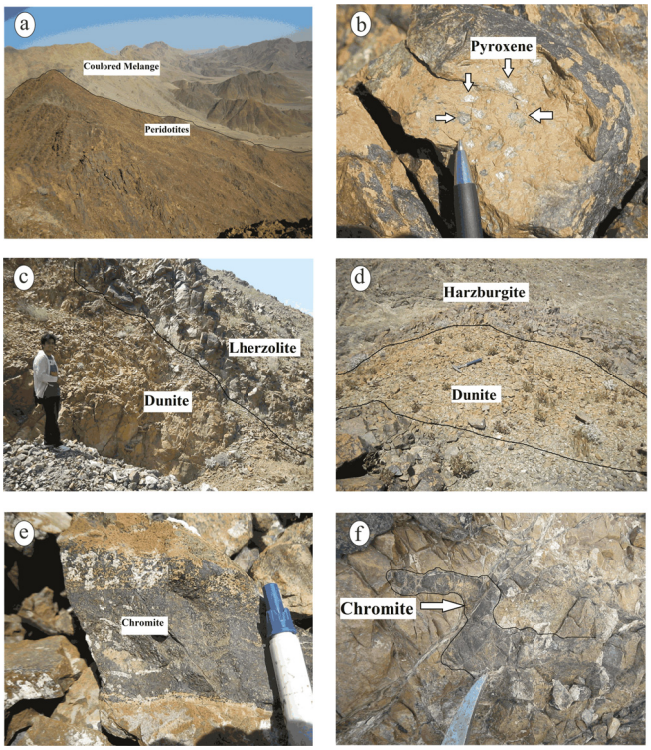

Figure 2. (a) General view of the Hadji-Abad Ophiolite.(b) Coarse-grainsed shiny orthopyroxenes on the surface of the harzburgites.(c) Sharp contact of dunites and lherzolites in Hadji Abad complex.(d) Lentiform dunites hosted by the harzburgites the studied complex.(e) Chromitite layer with a massive to dessimanted texture in the dunites.(f) Displacement of chromitite layer by faulting.

focuses on the mineral chemistry of the ultramafics (dunite, harzburgites and lherzolites), only these rocks are studied. According to field studies, the ultramafic part of the Hadji-Abad complex includes the harzburgite, lherzolite, dunite and chromitite. Reddish-brown coloured harzburgites, make up the large part of the complex and form a discontinuous and irregular layering with the dunites and lherzolites. The harzburgites mainly composed of olivine which is not recognizable in the field, but the pyroxene grains are more prominent because of their higher resistance and their shiny appearance. The orthopyroxene crystals with up to 1 cm in diameter show smooth and brilliant surface ([Fig. 2. b) and sometimes reveal a clear preferential orientation. Spinels in these rocks are observed as small and scattered crystals that sometimes show stretch elongation and lineation. Field characteristics of yellow to orange-coloured lherzolites are similar to those of the harzburgites, but they are more fine-grained. This unit is invaded by magnesite veins and shows a weak layering in which the lherzolites are alternatively placed alongside the dunites with faulted contacts (Fig. 2. c). Hadji-Abad yellow coloured dunites are found both in the form of discontinuous layers (up to 10 meters in length and 2 meters in thickness) and in the form of irregular masses up to 1 meter in diameter. These rocks host the chromitites of the Hadji-Abad complex and a lot of faults and fractures are developed in them in different directions (Fig. 2 d). Chrome Spinel is found as very small grains in most lithological units such as the harzburgites, lherzolites and dunites, however, in chromitites, chrome-spinel along with olivine, is considered as the main mineral of the rock units. In the Hadji-Abad complex, chromitites occur as two shapes: the first one is fine-grained and disseminated (0.1 to 2 mm in diameters) crystal set in layers with up to 10 cm in thickness (for example in the points: 28°21'34.03"N-\56°4'50.06"E, 28°21'97.03"N-56°4'50.98"E). The second one is found as thin layers with a maximum thickness of 8 cm containing coarse-grained chromite (more than 5 mm in diameters). This shape of chromitite occurs as alternative layers with the dunites and in some places, (for example points: 28°20'39.81"N-56°1'36.92"E. 28°21'56.98"N-56°4'40.04"E) chromite-rich layers and olivine bearing chromitite layers with sharp to gradual contacts (Fig. 2 e-f) occur.

Petrography

Harzburgite: More than 90 vol% of Hadji-Abad complex is made by the harzburgites and their average modal compositions are 70-80 vol% olivine, 20-30 vol% orthopyroxene and minor minerals including 1-3 vol% of clinopyroxene and up to 2 vol% spinel. The main texture of these rocks is proto-granular to porphyroclastic and there are different generations of minerals in them. First generation olivine (Ol1) mainly shows porphyroclastic texture and mechanical twining. Moreover, evidence of grain boundary migration can be observed in these rocks. In this case, boundaries between these large crystals (up to 1cm in diameter) are curved and irregular due to the dynamic recrystallization (Fig. 3 a and g). In some cases, these olivines have been converted into smaller olivine crystals (second generation, Ol2) and sometimes show a stretching and undulatory extinction. Undeformed fine-grained olivine (Ol2) crystals occur around or among orthopyroxene porphyroclasts. These olivines are found as fine-grained rocks and penetrate into coarse-grained orthopyroxene crystals and have created sinusoidal and irregular boundary around the hosted orthopyroxene crystals. Third generation fine-grained olivine (Ol3) is located between the large olivines and orthopyroxenes. They have polygonal shapes with triple junction boundaries and lack of any deformation features. The first-generation orthopyroxenes (Opx1) are large porphyroclasts with up to 1 cm in size and contain deformational features such as slightly folded, kink bond, undulatory extinction, clinopyroxene exsolution lamellae and elongation (Fig. 3. b). Second generation orthopyroxene (Opx2) crystallized as mosaic textured crystals with an approximate of 120° triple junctions without any deformation evidences (Fig. 3. c). Clinopyroxenes occur as smaller grains and fill the spaces between orthopyroxene and/or olivine grains, and as fine exsolution lamellae within the orthopyroxenes. Spinel is seen in two shapes in the harzburgites: The first one (Sp1) occurs as subhedral to euhedral coarse- grained grains which have been crystallized around olivines and orthopyroxenes. This group contains small olivine and orthopyroxene inclusions. The second one is found as anhedral crystals and fill between orthopyroxene and olivine grains.

Lherzolite: The Hadji-Abad mantle lherzolites contain 65-70 vol% olivine, 15-20 vol% orthopyroxene, 10-14 vol% clinopyroxene and about 1-2 vol% spinel. Petrographically, the lherzolites are very similar to the harzburgites and also contain various generations of olivine, orthopyroxene, clinopyroxene and spinel. The only difference is that the clinopyroxenes in these lherzolites, like orthopyroxenes, are seen in two shapes: The first one (Cpx1) is coarse-grained crystals with up to 3 mm in size. They exhibit deformation evidences and show curved boundaries filled by olivine, spinel or orthopyroxene (Fig. 3. e). The second group (Cpx2) is anhedral and intergranular grains found around the

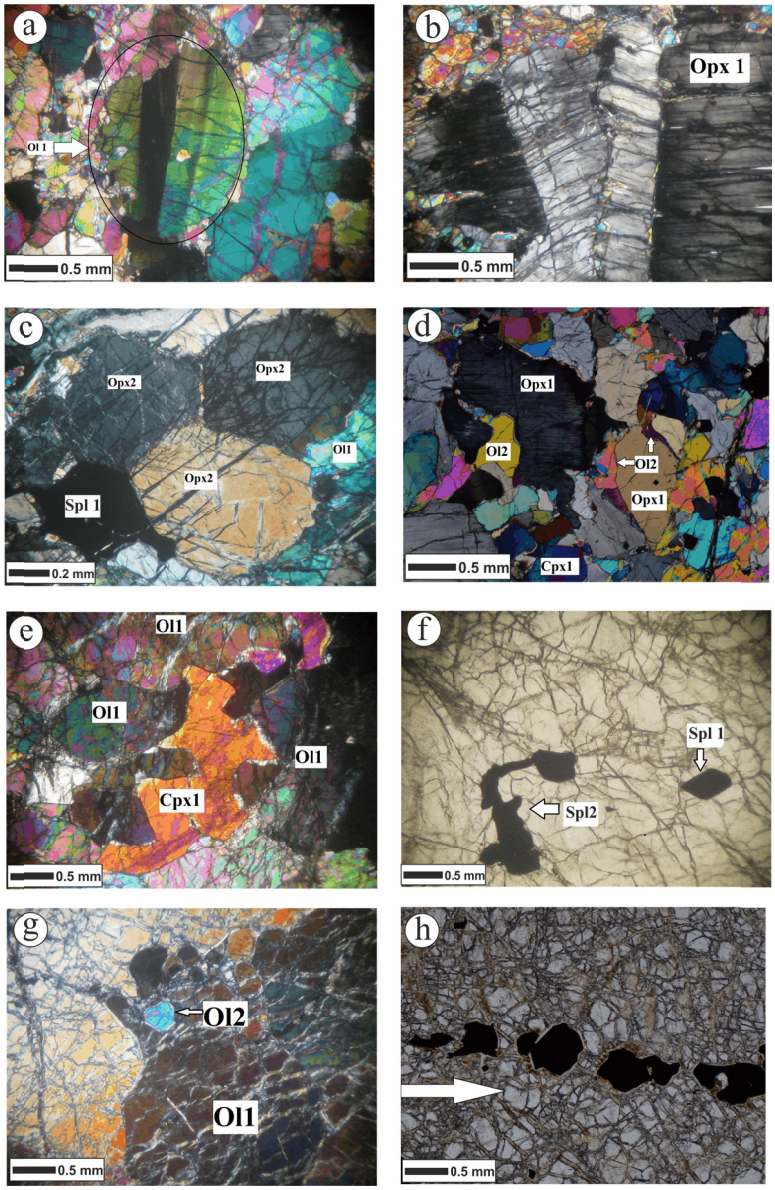

Figure 3. (a) The first-generation olivine of of Hadj-abad harzburgites with mechanical twin (b) The first-generation orthopyroxenes contain kink band. (c) Second-generation harzburgitic orthopyroxenes. (d) Second-generation olivines among the pyroxenses in the studied lherzolites. (e)lherzolitic clinopyroxenes, which crystallized among the other crystals.(f) Two generations of cr-spinels in the Hadji-Abad lherzolites. (g) Olivine neoblasts within the deformed olivines. (h) Cr-spinel array in disseminated chromitites.

orthopyroxene crystals without any deformation effects. In the lherzolites, spinels also occur as two shapes: the first shape is independent euhedral crystals with up to 1 mm in size which crystallized within the olivines. It seems that these crystals have not undergone severe deformation, because they have retained their original crystalline form. These spinels are dark brown in color and rarely contain olivine inclusions. The second group spinels (Sp2) are seen as anhedral grains with up to 3 mm in size and crystallized between olivine and clinopyroxene grains (Fig. 3. f). These spinels are light brown in color and have olivine inclusions.

Dunite: The Hadji-Abad dunites contain more than 97 vol% olivine about 3 vol% spinel. The original texture is granular, but mesh texture is also seen in strongly serpentinized dunites. Olivine can be seen in two forms; one occurs as large crystal with a maximum size of 4 mm as anhedral irregular shaped grains which

are strongly serpentinized in most cases. They represent a granular texture in dunites. These olivines show remarkable re-crystallization evidence and grain boundary migration recrystallization features, so that their boundaries are irregular and curve and interdigitated. They display the high-temperature deformation features. The second type of olivines are found as fine-grained crystals without any undulatory extinctions. These could be the result of recrystallization of deformed olivines in which the boundaries between the olivines show triple junction with a 120-degree with a mosaic texture. These crystals are smaller (with a size of 1 mm) and show no evidence of high-pressure and temperature deformation and they may have been formed due to recrystallization of the first olivines in crustal conditions (Fig. 3. g). The spinel is found as euhedral to subhedral grains. Their sizes reach up to 0.5 millimeter and is disseminated between the olivines or at their boundaries. In some dunites, cr-spinel crystals contain a pull apart cracks and weak lineation. Cr-spinels in the dunites are darker than the those in the lherzolites and harzburgites.

Chromitite: Hadji-Abad chromitites contain more than 75 vol% anhedral to subhedral chromite grains (with 2 to 4 mm in size) and represent disseminated to massive texture in which the chromites set in an serpentinized matrix. Chromite crystals are found at the boundaries between olivine grains and inside them and sometimes contain olivine and serpentine inclusions. They sometimes form massive textures chromitite layers between the dunites and sometimes as disseminated crystals in olivines. These types of chromitites do not display high-temperature deformation evidence; their grains are relatively undeformed and have not been stretched (Fig. 3. h). In other word, the textures in these chromitites are the same as cumulates from the magma, textures such as disseminated and massive textures which could have been formed as a result of crystallization and accumulation of chromite from a crystallized magma.

Mineral Chemistry

Spinel: Representative chemical analyses of chrome-spinels from different units of the Hadji-Abad complex are given in Table 1. In cr-spinels of the Hadji-Abad harzburgites, Cr# content [100×(Cr/(Cr+Al))] varies from 44 to 64 and the TiO_2 content vary from 0.01 to 0.1. The content of Al_2O_3 in these chromium spinels is relatively low and varies from 19.12 to 32.15 wt%. In these minerals, Mg#=[100×(Mg /(Mg+Fe^{2+}))] varies between 56.70 and 66.15. According to the results of the microprobe, some variations are observed from the core to the rim in the cr-spinels. Their centers are richer in Al_2O_3 and depleted in TiO_2, Mg# and Cr#. In the cr-spinels from lherzolites, there are some variations from core-to-rim, so that the amounts of Al_2O_3, TiO_2 and

Table 1. Representative analyses of different spinel shapes from Hadji-Abad ultramafic complex. (Hz: Harzburgite, Lz: Lherzolite, Du: Dunite, Chr: Chromitite)

Sample	C-11	C-11	C-6	C-33	C-33	C-1	C-1	C-51	C-51	C-15	C-15	A-3	C-45	C-45	C-45	C-7
Rock	Hz	Hz	Hz	Hz	Hz	Lz	Lz	Lz	Lz	Du	Du	Du	Chr	Chr	Chr	Chr
Mineral	sp	sp	sp	sp	sp	sp	sp	sp	sp	Sp	Sp	Sp	Sp	Sp	Sp	Sp
	Core	Rim		Core	Rim			Core	Rim	Core	Rim					
SiO_2	0.67	0.00	0.00	0.00	0.00	0.00	0.41	0.00	0.00	0.00	0.00	0.00	0.50	0.00	0.00	0.00
TiO_2	0.02	0.08	0.02	0.06	0.07	0.04	0.02	0.03	0.07	0.13	0.12	0.12	0.13	0.06	0.13	0.23
Al_2O_3	31.37	30.99	19.83	23.55	22.87	31.79	30.10	26.63	28.36	20.14	19.34	6.48	7.85	8.12	8.55	9.61
Cr_2O_3	36.67	38.00	49.02	44.67	45.20	39.16	39.75	42.21	40.86	52.24	52.31	58.48	62.03	61.65	62.07	61.45
FeO	15.83	16.42	18.20	17.69	16.40	14.02	15.17	18.79	17.97	15.21	18.11	28.49	17.26	19.78	17.28	17.70
MnO	0.27	0.19	0.35	0.25	0.26	0.20	0.30	0.24	0.34	0.26	0.38	0.52	0.34	0.39	0.35	0.29
MgO	14.99	14.30	12.00	13.69	13.88	15.51	15.66	13.78	13.90	14.06	12.78	6.54	11.99	10.67	12.30	12.57
CaO	0.06	0.03	0.02	0.01	0.00	0.01	0.05	0.01	0.02	0.00	0.02	0.00	0.00	0.02	0.02	0.02
NiO	0.04	0.09	0.01	0.08	0.12	0.12	0.14	0.08	0.13	0.06	0.36	0.02	0.07	0.02	0.07	0.08
TOTAL	99.92	100.10	99.45	100.00	98.80	100.85	101.60	101.77	101.65	102.10	103.42	100.65	100.17	100.71	100.77	101.94
Cation (Structural Formula on the basis of 32 Oxygen)																
Si	0.16	0.00	0.00	0.00	0.00	0.00	0.10	0.00	0.00	0.00	0.00	0.00	0.13	0.00	0.00	0.00
Ti	0.00	0.01	0.00	0.01	0.01	0.01	0.00	0.01	0.01	0.02	0.02	0.03	0.03	0.01	0.03	0.04
Al	8.65	8.60	5.87	6.76	6.64	8.68	8.21	7.44	7.87	5.75	5.52	2.08	2.43	2.52	2.62	2.89
Cr	6.79	7.07	9.73	8.60	8.80	7.17	7.27	7.91	7.61	10.00	10.02	12.61	12.86	12.83	12.75	12.41
Fe(iii)	0.24	0.30	0.39	0.63	0.54	0.13	0.33	0.65	0.50	0.20	0.41	1.26	0.40	0.63	0.59	0.60
Fe(ii)	2.86	2.93	3.43	2.98	2.84	2.59	2.60	3.07	3.04	2.88	3.26	5.24	3.38	3.73	3.17	3.18
Mn	0.05	0.04	0.07	0.05	0.05	0.04	0.06	0.05	0.07	0.05	0.08	0.12	0.08	0.09	0.08	0.06
Mg	5.23	5.02	4.49	4.97	5.10	5.36	5.40	4.87	4.88	5.08	4.62	2.66	4.69	4.19	4.76	4.79
Ca	0.02	0.01	0.01	0.00	0.00	0.00	0.01	0.00	0.01	0.00	0.01	0.00	0.00	0.01	0.01	0.01
Ni	0.01	0.02	0.00	0.01	0.02	0.02	0.02	0.01	0.02	0.01	0.06	0.00	0.01	0.00	0.01	0.01
TOTAL	24.00	24.00	24.00	24.00	24.00	24.00	24.00	24.00	24.00	24.00	24.00	24.00	24.00	24.00	24.00	24.00
Fe/Fe+Mg	0.37	0.39	0.46	0.42	0.40	0.34	0.35	0.43	0.42	0.38	0.44	0.71	0.45	0.51	0.44	0.44
Cr#	44.00	45.00	62.00	56.00	57.00	45.00	47.00	52.00	49.00	64.00	64.00	86.00	84.00	84.00	83.00	81.09
Mg#	64.69	63.11	56.70	62.55	64.21	67.45	67.47	61.29	61.63	63.79	58.64	33.66	58.09	52.91	60.06	60.11

Mg# increase from the cores to the rims, while Cr# is decreased. In cr-spinels of the lherzolites, Cr# is about 45 to 52. They have lower Cr# values compared with the harzburgites. The Mg# contents in these cr-spinels vary from 58.85 to 68.34 which is higher than those in the harzburgites. The amounts of TiO_2 in the cr-spinels of lherzolites reach up to 0.08 and the Al_2O_3 content varies from 26.42 to 32.59. Compositionally, cr-spinels from the dunites are more enriched in chromium and their Cr# content varies from 63 to 86. In these crystals, the content of Al_2O_3, Mg# and TiO_2 change 6.48 to 20.33, 33.66 to 63.79 and 0.08 to 0.25, respectively. Some of the significant features of cr-spinels from dunites are the high Cr# content and low Al_2O_3 content. Their amount of Cr# ranges from 80 to 84, while Al_2O_3 is lower than other cr-spinels and varies from 7.5 to 10.13%. The Mg# content in these crystals is high and varies from 47.96 to 62.90. Chromites from chromitites are more enriched in TiO_2 than the rest of the peridotites and varies from 0.06 to 0.35 wt%. The chemical composition of chromites in Hadji-Abad chromitites in Cr_2O_3-TiO_2 diagram fall in podiform chromitite field (Fig. 4. a). Besides, all types of chrome-spinels from Hadji-Abad lithologies exhibit negative correlations in Cr_2O_3-Al_2O_3 diagram and plot in the mantle array spinel field (Fig. 4. b).

Olivine: Olivines are the most abundant minerals in Hadji-Abad peridotite rocks. The chemical composition of these minerals is shown in Table 2. The relative content of Fo [Fo =100×(Mg /(Mg+Fe^{2+})] in the olivines of harzburgites range from 85.88 to 93.22. In these minerals, NiO varies from 0.22 to 0.46 and MnO changes from 0.06 to 0.19, mostly in the range of mantle arrays. The amount of Fo in olivines of the lherzolites range from 90.92 to 92.69, while their NiO contents vary from 0.38 to 0.46 and MnO content in these olivines varies from 0.05 to 0.18 which are approximately the same as olivines of the harzburgites. The olivines from dunites show a small variation in the amount of Fo, (92.60 to 93.77). They have the lowest content of NiO compared to other olivines, (0.02 to 0.46). The MnO content in these olivines also varies from 0.05 to 0.20. Olivine composition of chromitites changes with chromite percentages. In addition, the Fo content in olivines from these rocks varies from 94.43 to 95.87. The more chromite content in the rock, the higher the content of Fo in the olivines. The NiO content in these rocks ranges from 0.37 to 0.57 and the olivines from the chromitites have the highest content of Fo and NiO compared with the other rocks. In Figure 5.a and b, most of olivines from the harzburgites and dunites fall in the field of mantle olivine array.

Orthopyroxene: The chemical compositions of the studied orthopyroxenes are shown in Table 3. They can be found in the harzburgites and lherzolites and entirely fall in enstatite field (Fig. 6. a). The orthopyroxenes of harzburgites have an En content of 87 to 91 and a Mg# content of 91.70 to 93.05 and their Al_2O_3 content varies from 0.02 to 2.63; while the Cr_2O_3 ranges from 0.02 to 2.34. The orthopyroxenes from lherzolites have less than the En content (86.21 and 90.21); while, their Mg# and Al_2O_3 vary from 91.54 to 92.53 and from 2.08 to 2.83, respectively which is higher than the harzburgites. The Cr_2O_3 content in these orthopyroxenes ranges from 0.63 to 0.93 which is less than those of harzburgites. In Mg-Al_2O_3 diagram (Fig. 6. b), most Hadji-Abad orthopyroxenes are located within the range of high-pressure pyroxenes.

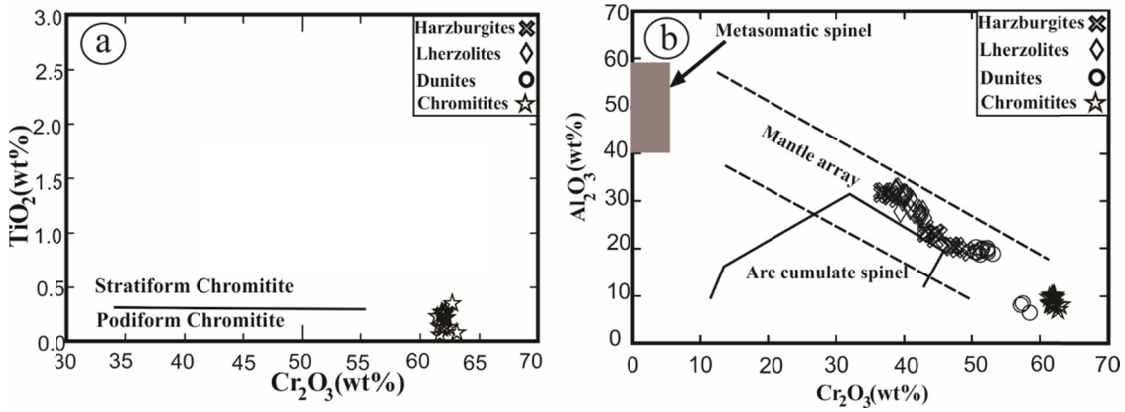

Figure 4. (a) Variations of Cr_2O_3 vs TiO_2 in the Hadji-Abad chromitite (quoted from Bonavia et al., [17]). The same symbols are shown in the following diagrams.(b) Variations of Al_2O_3 vs Cr_2O_3 in cr-spinels from the Hadji-Abad peridotites. (Fields from Kepezhinskas, [18]).

Table 2. Representative chemical analyses of olivines from Hadji-Abad complex

Sample	C11	C-6	C-33	C-1	C-1	C-1	A-3	A-3	A-3	A-3	C-7	C-7	C-45	C-45	C-45	C-45
Rock	Hz	Hz	Hz	LZ	LZ	LZ	Du	Du	Du	Du	Ch	Ch	Ch	Ch	Ch	Ch
Mineral	Ol	Ol	Ol	Ol	Ol	Ol	Ol	Ol	Ol	Ol	Ol	Ol	Ol	Ol	Ol	Ol
SiO_2	42.76	42.17	41.63	41.27	41.38	41.46	41.72	41.73	42.00	42.13	42.05	41.95	41.97	42.18	41.30	41.15
TiO_2	0.00	0.01	0.00	0.00	0.00	0.02	0.00	0.00	0.00	0.00	0.00	0.01	0.00	0.00	0.00	0.00
Al_2O_3	0.00	0.00	0.00	0.00	0.01	0.00	0.04	0.00	0.01	0.00	0.02	0.00	0.01	0.00	0.00	0.00
Cr_2O_3	0.00	0.00	0.00	0.00	0.00	0.01	0.03	0.01	0.00	0.01	0.01	0.01	0.00	0.03	0.01	0.00
FeO	8.80	6.52	7.75	8.12	7.99	7.70	6.84	6.44	6.32	6.16	4.79	5.13	4.18	4.12	4.57	4.75
MnO	0.17	0.11	0.10	0.05	0.20	0.18	0.15	0.12	0.05	0.06	0.09	0.04	0.11	0.03	0.00	0.08
MgO	49.05	51.12	50.63	51.26	51.46	51.20	52.63	52.58	52.54	52.47	53.79	53.45	54.20	54.04	53.36	54.03
NIO	0.22	0.35	0.40	0.43	0.46	0.42	0.46	0.40	0.38	0.36	0.53	0.53	0.43	0.48	0.37	0.39
CaO	0.01	0.02	0.03	0.00	0.01	0.03	0.04	0.04	0.04	0.10	0.01	0.04	0.01	0.00	0.04	0.07
Total	101.01	100.30	100.54	101.13	101.51	101.02	101.91	101.34	101.34	101.28	101.29	101.16	100.91	100.88	99.65	100.47
Cation (Structural Formula on the basis of 4 Oxygen)																
Si	1.02	1.01	1.01	0.99	0.99	1.00	0.99	1.00	1.00	1.00	1.00	1.00	1.00	1.00	0.99	0.98
Ti	0.00	0.00	0.00	0.00	0.00	0.00	0.00	0.00	0.00	0.00	0.00	0.00	0.00	0.00	0.00	0.00
Al	0.00	0.00	0.00	0.00	0.00	0.00	0.00	0.00	0.00	0.00	0.00	0.00	0.00	0.00	0.00	0.00
Cr	0.00	0.00	0.00	0.00	0.00	0.00	0.00	0.00	0.00	0.00	0.00	0.00	0.00	0.00	0.00	0.00
Fe	0.25	0.13	0.16	0.16	0.16	0.16	0.14	0.13	0.13	0.12	0.10	0.10	0.08	0.08	0.09	0.10
Mn	0.00	0.00	0.00	0.00	0.00	0.00	0.00	0.00	0.00	0.00	0.00	0.00	0.00	0.00	0.00	0.00
Mg	1.74	1.83	1.82	1.84	1.84	1.84	1.87	1.87	1.87	1.86	1.90	1.89	1.92	1.91	1.91	1.93
Ni	0.00	0.01	0.01	0.01	0.01	0.01	0.01	0.00	0.00	0.01	0.01	0.01	0.01	0.01	0.01	0.01
Ca	0.01	0.00	0.00	0.00	0.00	0.00	0.00	0.01	0.01	0.00	0.00	0.00	0.00	0.00	0.00	0.00
Total	3.02	2.99	3.00	3.01	3.01	3.00	3.01	3.01	3.01	3.00	3.00	3.00	3.01	3.00	3.01	3.02
Fo	88.85	93.22	92.00	91.79	91.80	92.05	93.07	93.46	93.64	93.77	95.16	94.85	95.75	95.87	95.42	95.22
Fa	10.98	6.67	7.90	8.16	8.00	7.77	6.78	6.42	6.31	6.17	4.75	5.11	4.14	4.10	4.58	4.70

Clinopyroxene: The chemical compositions of the Hadji-Abad clinopyroxenes are presented in Table 4. They are diopside-type (Fig. 6. a) and their En contents change from 47.80 to 60.40 while, their Wo and Fs contents vary from 38.90 to 48.90, and 2.10 to 6, respectively. In these clinopyroxenes, the Mg# is relatively high (91 to 98.8); while Al_2O_3 ranges from 1.61 to 3.18. Additionally, Na_2O varies from 0.01 to 0.1 and Cr_2O_3 varies from 0.59 to 1.29. In these clinopyroxenes, the FeO (from 1. 53 to 2.23) and TiO_2 (0.02 to 0.07) contents are relatively low. Clinopyroxenes from lherzolites have En content ranging from 48.60 to 53.50, the Wo, Fs and Mg# content vary from 34.30 to 48.50, 1 to 4.2 and 92.4 to 95.7, respectively. Their Al_2O_3, Na_2O and Cr_2O_3 contents vary from 1.49 to 3.10, 0 to 0 .14 and 0.51 to 1.1, respectively. Plotting of these clinopyroxenes on the Mg#-Al_2O_3 diagram shows the range of high pressure clinopyroxenes (Fig. 6. b).

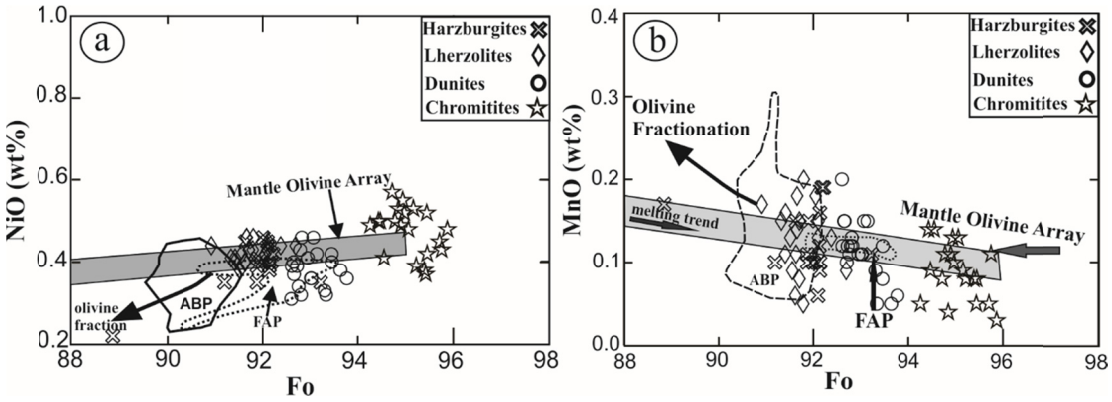

Figure 5. (a) Variations of Fo vs NiO in the olivines present in different rocks of the study area compared to the mantle olivine array [19]. Partial melting and fractionation trends (from Ozawa, [20]), ABP=Abyssal peridotites and FAP= Fore arc peridotites (from Page et al., [21]). (b) Fo vs MnO diagram for the olivines present in different rocks of the study area compared to the mantle olivine array [19]).

Table 3. Representative analyses of orthopyroxenes from Hadji-Abad complex.

Sample	C-11	C-11	C-11	C-11	C-11	C-11	C-6	C-6	C-33	C-33	C-1	C-1	C-1	C-1	C-1	C-51
Rock	Hz	Hz	Hz	Hz	Hz	Hz	Hz	Hz	Hz	Hz	Lz	Lz	Lz	Lz	Lz	Lz
Mineral	Opx	Opx	Opx	Opx	Opx	Opx	Opx	Opx	Oox	Oox	Opx	Opx	Opx	Opx	Cpx	Opx
SiO_2	57.29	57.18	57.02	57.18	57.30	57.77	58.51	58.33	56.79	57.76	56.53	56.81	56.85	56.95	57.53	58.05
TiO_2	0.03	0.02	2.34	2.18	0.06	0.02	0.03	0.00	0.02	0.00	2.83	2.39	2.41	0.03	0.00	2.12
Al_2O_3	2.63	2.66	0.02	0.03	2.34	2.21	1.27	1.40	1.99	1.76	0.00	0.03	0.00	2.38	2.33	0.03
Cr_2O_3	0.77	0.72	0.70	0.71	0.65	0.60	0.45	0.61	0.73	0.50	0.84	0.69	0.63	0.64	0.62	0.67
FeO	5.17	5.41	5.00	5.40	5.37	5.34	4.66	5.19	5.06	5.10	5.40	5.23	5.68	5.25	5.14	5.04
MnO	0.13	0.11	0.18	0.15	0.11	0.13	0.16	0.08	0.16	0.18	0.15	0.14	0.15	0.11	0.09	0.12
MgO	34.36	34.61	34.12	34.52	33.88	34.40	35.04	35.11	34.19	34.77	33.87	33.95	34.55	34.58	34.70	35.08
CaO	0.86	0.82	1.47	1.04	1.47	1.30	1.54	0.85	0.74	0.80	2.01	1.57	1.05	1.26	1.49	1.01
Na_2O	0.01	0.00	0.00	0.01	0.00	0.00	0.00	0.01	0.00	0.01	0.00	0.00	0.00	0.00	0.00	0.00
K_2O	0.00	0.00	0.00	0.00	0.00	0.00	0.00	0.00	0.00	0.00	0.00	0.00	0.00	0.00	0.00	0.00
Total	101.25	101.54	100.85	101.22	101.19	101.76	101.65	101.57	99.68	100.88	101.63	100.81	101.32	101.20	101.90	102.12
Cation (Structural Formula on the basis of 6 Oxygen)																
Si	1.94	1.94	1.95	1.95	1.95	1.98	1.97	1.96	1.97	1.95	1.95	1.95	1.94	1.94	1.96	
Ti	0.00	0.00	0.06	0.06	0.00	0.00	0.00	0.00	0.00	0.00	0.00	0.00	0.00	0.00	0.00	0.05
Al	0.11	0.11	0.00	0.00	0.09	0.09	0.05	0.06	0.08	0.07	0.08	0.08	0.08	0.10	0.09	0.00
Cr	0.02	0.02	0.02	0.02	0.02	0.02	0.01	0.02	0.02	0.01	0.02	0.02	0.02	0.02	0.02	0.02
Fe++	0.15	0.15	0.14	0.15	0.15	0.15	0.15	0.15	0.15	0.15	0.14	0.16	0.15	0.15	0.15	0.14
Mn	0.00	0.00	0.01	0.00	0.00	0.00	0.00	0.00	0.00	0.01	0.00	0.01	0.01	0.00	0.00	0.00
Mg	1.74	1.74	1.74	1.76	1.72	1.72	1.77	1.77	1.76	1.76	1.76	1.75	1.75	1.75	1.75	1.77
Ca	0.03	0.03	0.05	0.04	0.05	0.05	0.06	0.03	0.03	0.03	0.04	0.04	0.04	0.05	0.05	0.04
Na	0.00	0.00	0.00	0.00	0.00	0.00	0.00	0.00	0.00	0.00	0.00	0.00	0.00	0.00	0.00	0.00
K	0.00	0.00	0.00	0.00	0.00	0.00	0.00	0.00	0.00	0.00	0.00	0.00	0.00	0.00	0.00	0.00
Total	3.99	3.99	3.98	3.98	3.99	3.99	4.00	3.99	3.99	3.99	4.00	4.00	4.00	4.01	4.00	3.98
En	0.90	0.90	0.87	0.88	0.88	0.88	0.89	0.90	0.90	0.90	90.21	90.17	89.78	90.60	90.00	87.80
Fs	0.09	0.08	0.11	0.10	0.09	0.09	0.08	0.09	0.09	0.08	7.92	7.92	8.14	7.00	7.20	10.30
Wo	0.02	0.02	0.03	0.02	0.03	0.03	0.03	0.02	0.01	0.01	1.87	1.91	2.09	2.40	2.80	1.80
Mg#	92.22	92.22	92.41	91.94	91.83	91.83	92.05	91.30	91.20	91.40	0.92	0.92	0.92	0.93	0.93	0.90

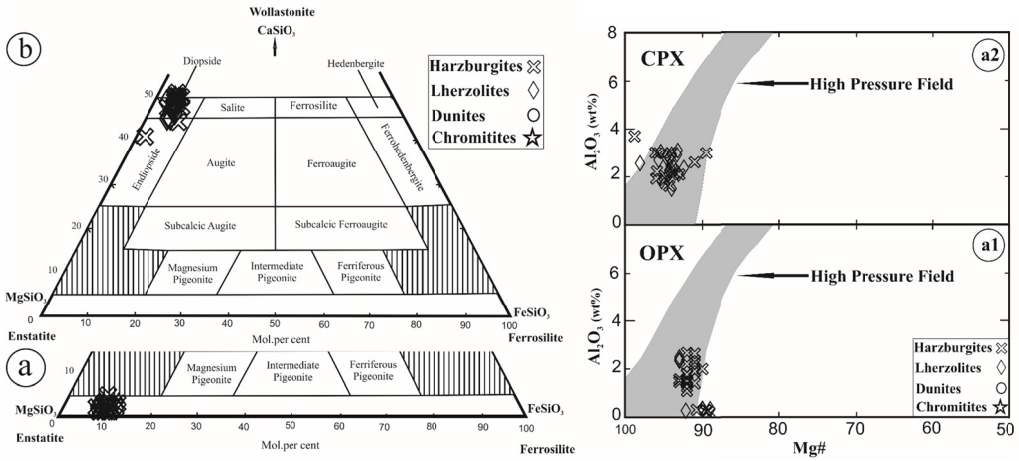

Figure 6. (a). The position of a: orthopyroxene and b: clinopyroxenes in the Hadji-Abad peridotites on the EN-Fs-Wo triangle [22]. (b). Mg# vs Al_2O_3 diagram for Hadji Abad (a1) orthopyroxenes and (a2) clinopyroxenes (High pressure range from Medaris, [23]).

Discussion

Field studies, petrography, mineralogy and chemical characteristics of minerals and whole rocks from Hadji-Abad peridotites revealed that they resemble to those mantle derived rocks. In order to clarify this complex history and tectonic setting in which the Hadji-Abad complex originated, in the following sections we try to estimate the degree of partial melting, calculate and estimate temperatures and pressures and detect tectonic settings as well as petrological evolutions of Hadji-Abad peridotites.

Partial melting

The modal composition and chemistry of minerals found in the mantle peridotites can be an indicator for the degree of partial melting or depletion of these rocks. Especially, the chemical composition of clinopyroxene in peridotites is a good indicator for evaluating partial melting event. During the partial melting and in anhydrated conditions, it rapidly melts and disappears. Modal amounts of clinopyroxene in the Hadji-Abad peridotites show that from the lherzolites toward the dunites, the partial melting increases, the amount of

Table 4. Representative analyses of clinopyroxenes from Hadji-Abad complex.

Sample	C-11	C-11	C-11	C-11	C-11	C-11	C-33	C-33	C-1	C-1	C-1	C-1	C-1	C-1	C-1	C-51
Rock	Hz	Hz	Hz	Hz	Hz	Hz	Hz	Hz	LZ	LZ	LZ	LZ	LZ	LZ	LZ	LZ
Mineral	Cpx	Cpx	Cpx	Cpx	Cpx	Cpx	Cpx	Cpx	Cpx	Cpx	Cpx	Cpx	Cpx	Cpx	Cpx	Cpx
SiO_2	53.4	53.6	53.4	54.5	54.8	53.4	54.5	54	53.39	53.89	53.72	53.5	53.5	53.6	53.5	55.2
TiO_2	0.05	0.08	0.07	0.07	0.06	0.05	0.06	0.03	0.02	0.03	0.06	0.02	0.02	0.09	0	0.02
Al_2O_3	3.18	3	3.01	2.99	1.61	2.99	2.09	2.21	3.05	2.92	3.10	2.94	2.8	2.81	2.92	2.1
Cr_2O_3	1.17	1.07	1.21	1.12	0.59	1.07	0.86	0.98	1.06	1.02	1.09	1.03	0.91	1.03	0.99	0.76
FeO	2.14	1.94	2.21	1.93	1.48	1.79	1.53	1.93	1.90	2.14	2.31	2.31	2.08	2.25	2.16	2.12
MnO	0.06	0.18	0.09	0.03	0.07	0.08	0.04	0.11	0.14	0.10	0.05	0.12	0.11	0.11	0.14	0.05
MgO	17.2	17.3	18.5	18.7	18	17.1	17.5	17.7	17.90	19.04	18.93	18.2	18.1	18.2	18.3	18.6
CaO	24	24	22.8	21.5	24.5	24.6	24.7	24.6	23.40	21.91	21.65	22.8	23	22.6	22.3	23.7
Na2O	0.05	0.06	0.08	0.07	0.04	0.1	0.01	0.04	0.06	0.08	0.05	0.04	0.05	0.14	0.07	0.01
K2O	0	0.02	0	0.02	0	0	0	0	0.00	0.01	0.02	0	0	0.03	0	0
Total	101	101	101	101	101	101	101	102	100.91	101.14	100.98	101	101	101	100	103
Cation (Structural Formula on the basis of 6 Oxygen)																
Si	1.92	1.92	1.91	1.95	1.96	1.92	1.96	1.93	1.917	1.924	1.922	1.92	1.93	1.93	1.93	1.95
Ti	0	0	0	0	0	0	0	0	0.001	0.001	0.002	0	0	0	0	0
Al	0.14	0.13	0.13	0.13	0.07	0.13	0.09	0.09	0.129	0.123	0.131	0.12	0.12	0.12	0.12	0.09
Cr	0.03	0.03	0.03	0.03	0.02	0.03	0.02	0.03	0.03	0.029	0.031	0.03	0.03	0.03	0.03	0.02
Fe3+	-0	0	0.03	-0.1	-0	0.01	-0	0.02	0.01	0.006	-0.005	0.01	0.01	0.01	-0	-0
Fe2+	0.07	0.06	0.04	0.12	0.06	0.04	0.07	0.04	0.047	0.058	0.074	0.06	0.05	0.06	0.07	0.07
Mn	0	0.01	0	0	0	0	0	0	0.004	0.003	0.002	0	0	0	0	0
Mg	0.92	0.93	0.98	1	0.96	0.92	0.94	0.94	0.958	1.013	1.01	0.97	0.97	0.97	0.98	0.98
Ca	0.92	0.92	0.87	0.83	0.94	0.95	0.95	0.94	0.9	0.838	0.83	0.88	0.89	0.87	0.86	0.9
Na	0	0	0.01	0.01	0	0.01	0	0	0.004	0.006	0.003	0	0	0.01	0.01	0
K	0	0	0	0	0	0	0	0	0	0	0.001	0	0	0	0	0
Total	4	4	4	4	4	4	4	4	4	4	4	4	4	4	4	4
En	48.1	48.6	51.9	51.4	49.1	48.1	47.8	49	50.3	53.1	52.8	50.9	50.8	51.2	51.3	50.3
Fs	3.7	3.1	2.1	6	2.9	2.2	3.6	2.1	2.4	3.1	3.9	3.2	2.8	3.1	3.7	3.7
Wo	48.2	48.4	46	42.5	47.9	49.7	48.6	48.9	47.3	43.9	43.4	45.9	46.4	45.7	45.1	46
Mg#	92.9	94.1	96.1	89.5	94.3	95.7	93	95.9	95.4	94.6	93.2	94	94.7	94.3	93.3	93.1

clinopyroxene in the rocks is reduced and the amount of modal olivine gradually increases. In the Hadji-Abad peridotites, the following evidences also suggest that these rocks have undergone a partial melting process: The petrography evidence such as lobate boundaries between olivine grains, the presence of fine-grained olivine crystals on the periphery and between the coarse crystals of orthopyroxene can indicative of incongruent melting of orthopyroxene as suggested by Page et al., [21]. Harzburgitic olivines have high forsterite contents (88.85 to 93.22) which are apparently seen in the olivines of the residual mantle. In addition, high amounts of NiO wt% in this mineral is a good indicator of partial melting [24]. Clinopyroxenes found in the Hadji-Abad peridotites are depleted in Al_2O_3 and Cr_2O_3 with high Mg# values which is an evidence for partial melting [21]. By comparing these available data with experimental data from Hirose and Kawamoto, [25], we found that the chemical composition of cr-spinel from the Hadji-Abad peridotites represents about 20% partial melting for the host harzburgites. Hirose and Kawamoto, [25], by partial melting of a natural lherzolite at 1 GPa and over the temperatures between 1100-1350 °C showed that in the partially melted lherzolite, the contents of Al2O3 and Cr2O3 of the studied cr-spinels were 14-34 w% and 36-42 w% respectively. These values for cr-spinels of the Hadji-Abad harzburgites are 22-31 and 36-42 respectively. In the log (TiO_2)-Cr# diagram (Fig. 7 a), the studied harzburgitic and lherzolitic cr-spinel fall in the field of depleted peridotites; while the disseminated chromites in the dunites along with the chromitites, fall in the field of those chromites which crystallize from the boninitic melts. In the Cr#-TiO_2 diagram (Fig. 7 b). the chemical compositions of these cr-spinels represent the partial melting of the host rocks. High contents of Cr# in the Hadji-Abad chromitites can be evidence of crystallization from high Mg# boninite melts [28]. The compositions of the cr-spinels of the dunites also indicate that the dunites are likely to be formed by the reaction of the boninite melts with a mantle which has undergone 15 to 20% partial melting. Both of these phenomena (15-20% partial melting and the performance of the boninite melts and the formation of chromitite and dunite have been reported in the suprasubduction zones [29]. Some evidences such as high Fo contents of the olivines and high Cr# values of spinels, besides textural features such as lobate boundaries in the first-generation olivines and pyroxenes of Hadji-Abad peridotites indicate that the harzburgite and lherzolites are refractory mantle rocks. These evidences indicate that at the very high T

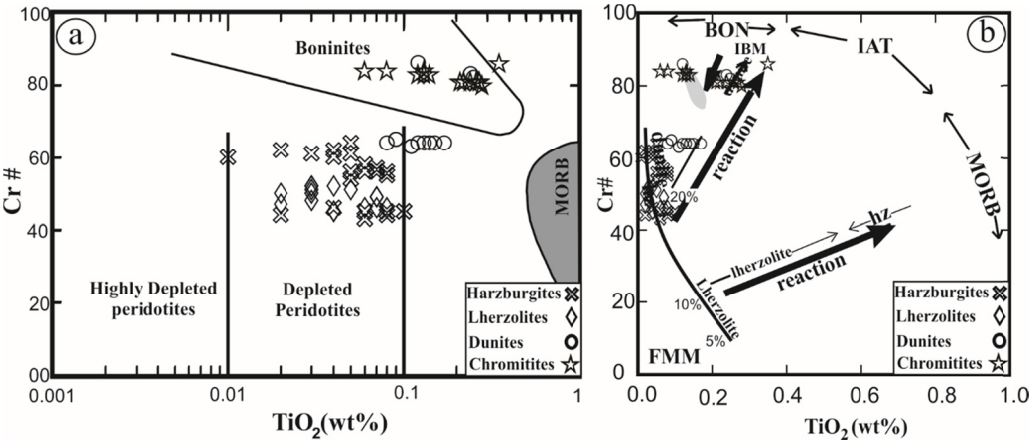

Figure 7. (a) TiO_2 vs Cr# diagram for cr-spinels from the study area; The boundaries presented by Dick and Bullen [26], (b) Cr# vs TiO_2 diagram for cr-spinels of the Hadji-Abad peridotites; (fields from Pearce et al., [27]). (FMM = fertile mantle, IBM = Iso-bonin Mariana, HZ = Harzburgite, Bon = Boninite).

conditions, first generation of olivines and cr-spinels crystallized concurrently, then the first generation of orthopyroxene and then clinopyroxene have been crystallized.

Geo-thermo-barometry

Subsolidus phase equilibria are the most common consequences of deformational events. Hadji-Abad peridotites have passed deformation phases and such processes have caused the temperatures obtained for different rocks of the Hadji-Abad peridotite complex which are not primarily the initial crystallization temperatures and, in some cases, the results refer to the subsolidous phase equilibria temperatures. These temperatures indicate that the studied rocks have been re-equilibrated in the crustal conditions after formation in the upper mantle. Petrographic evidence also confirms the existence of exsolution lamella within orthopyroxene and clinopyroxenes, the presence of the second and third generation of minerals, mosaic textures, the presence of a triple junction between them and the presence of olivine neoblasts (Ol2), all testify to the re-equilibration of these rocks in the crust. The presence of olivines, orthopyroxene, clinopyroxene and spinel in the studied peridotites and the presence of coexisting Orthopyroxene-clinopyroxene as well as olivine-spinel based on petrographic evidence can be used for geothemobarometric calculations. Using a single-clinopyroxene geo-thermometer [30], the equilibrium temperature for clinopyroxenes in the studied harzburgites and lherzolites varies from 750 to 1118 °C by the following equation:

$T\ (^{o}K) \pm 30 = 23166\ (\pm 447) + 39.28\ (\pm 4.27).\ P\ (kbar) / [13.25\ (\pm 0.32) + 15.32\ (\pm 2.90).\ Ti + 4.50\ (\pm 0.83).\ Fe - 1.55\ (\pm 0.29).\ (Al + Cr - Na) + (\ln a_{en}^{Cpx})^2]$

$a_{en}^{Cpx} = (1 - Ca - Na - K).\ [1 - 1/2\ .(Al + Cr + Na + K)]$

Using the geo-thermometer of orthopyroxene-clinopyroxene ([31]; Ca in orthopyroxene) in the harzburgites and lherzolites, it was found out that the temperatures range from 936 to 1182 °C by the following equation:

$T\ ^{\circ}C = [23664 + (24.9 + 126.3\ X_{fe}^{cpx}).P_{kbar} / 13.38 + (\ln k_{D}^{*})^2 + 11.59\ X_{fe}^{opx}] - 273.15$

$KD^{*} = (1 - N_{ca}^{cpx} / (1 - N_{Na}^{cpx})) / (1 - N_{ca}^{opx} / (1 - N_{Na}^{opx}))$

On the other hand, the temperature is estimated to be 1182 to 1292 °C using Fe-Mg contents in orthopyroxene of harzburgites and lherzolites of the Hadji-Abad complex and the equation [32]:

$T\ ^{\circ}C = (7341 / 3.355 + 2.44\ .\ X_{Fe}^{opx} - \ln k) - 273.15$

$X_{Fe}^{opx} = Fe^{2+} / Fe^{2+} + Mg^{2+}$

This range of temperature reports by Ionov et al., [33] for the Siberain peridotites. The changes in temperature estimates seen in Geothermometric calculations are due to the fact that microprobe electron analyzes have been performed on different generations of minerals.

Tectonic environment

Different tectonic settings are introduced for the formation and emplacement of mantle peridotites. Some of them are considered as deep peridotites in the ocean floor basins [34]. This type is often composed of spinel lherzolites formed by partial melting of 5-15% in dehydrated conditions, but peridotites related to mantle areas over the subduction zones are dominated by spinel harzburgites and dunites which are the result of over 20% of the hydrous partial melting events [35, 5, 36].

Since Ti content in clinopyroxene reflects the degree of depletion and partial melting of the source rock and it also indicates the activity of Ti in the parent magma of the magmatic rocks [37], it can be concluded that these types of ultramafic rocks in the ophiolites, have affected by partial melting, and the Ti contained therein has been entered into the magma. The main part of the Hadji-Abad ultramafic is formed by spinel harzburgites and dunites. Therefore, it is possible for them to form in a suprasubduction zone. In order to testify this hypothesis, we used tectonic and mineralogical evidences and evaluated them for the studied peridotites.

The Zagros ophiolitic belt forms a part of the Tethys ophiolite belt which extends from Cyprus to Oman. The formation of these ophiolites is a result of the processes related to the subduction zone [38, 39, 40, 2, 41]. The Zagros thrust ophiolite belt divides into two groups of outer and inner ophiolites. The Esfandagheh-Hadji-Abad ophiolitic belt which hosts the studied Hadji-Abad complex, is a part of the outer Zagros ophiolites [42, 15, 12, 43]. There are different views on the formation and tectonics of the Esfandagheh-Hadji-Abad ophiolite belt: Shafaii Moghaddam et al., [44] believe that the ophiolites of this region are the remnants of the Neothetys oceanic lithosphere in the central Iran which is formed during the Neothetys subduction in the upper Cretaceous in the central Iran. Shafahi Moghaddam et al, [13] argue that the late Cretaceous ophiolites located in central southern Iran, including the Peri-Arabian ophiolites and the Zagros ophiolites are derived from the southern Tethys subduction. Peyghambari et al., [9] by using various geochemical evidences, believes that Deh Sheikh ophiolite complex is part of the oceanic lithosphere located in the suprasubduction zone. This complex also forms a part of the Esfandagheh-Hadji-Abad ophiolite belt. Ahmadipour and shahabpour [45] also attribute the ophiolites of the Esfandagheh region to processes related to the Neotethys subduction zone below the Sanandaj-Sirjan zone, as a result, a back arc is formed between the Sanandaj-Sirjan zone and the central Iranian micro-continent. During the Cretaceous period, the Sanandaj-Sirjan region acted as an arc island. This situation can be linked to petrological processes which are commonly carried out in the upper subduction zone. According to Mercier and Nicholas [46], the Fo content of cumulate olivines varied between 86-88, while it ranged from 91 to 92 in the mantle olivines. Therefore, given the high Fo content in the olivines from the studied dunites, it can be inferred that some of these rocks belong to the mantle. The chemical compositions of coexisting olivines and spinels found in the Hadji-Abad peridotites which are plotted on the Fo olivine–Cr# spinel diagram (Fig. 8 a), demonstrate an increasing melting trend which is consistent with a suprasubduction zone setting. In Al_2O_3-TiO_2 diagram (Fig. 8 b), the existing cr-spinels found in the harzburgites and lherzolites plot within the common range between the peridotites of the suprasubduction zone and the MORBs. Additionally, chemical compositions of Hadji-Abad clinopyroxenes confirm the suprasubduction peridotite for Hadji-Abad peridotites (Fig. 9). Since the mineral chemistry data of Hadji-Abad complex fall in the MORB field in Figure 8 b, and in the suprasubduction zone field in Figures 8 a and 9,

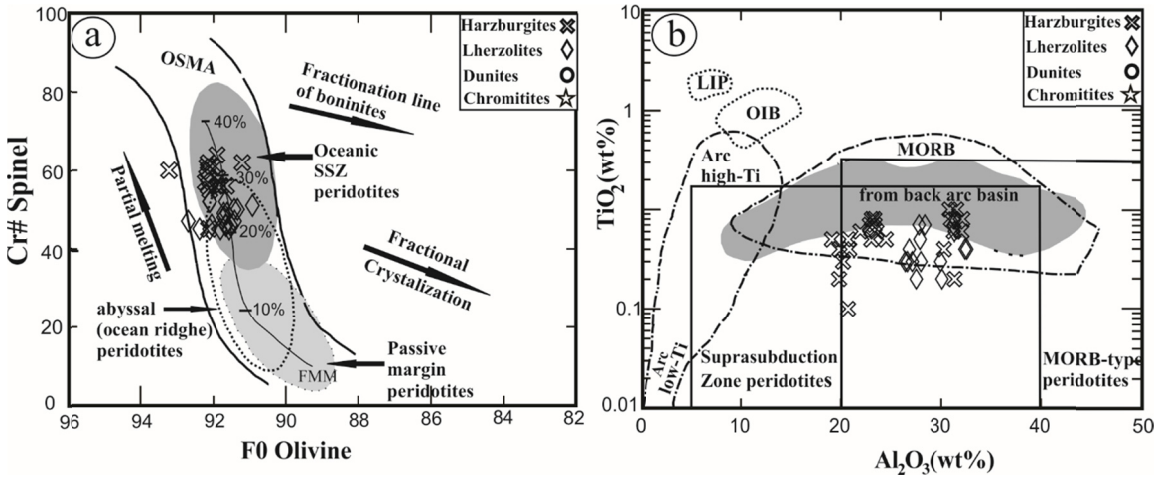

Figure 8. (a). Relationship between Cr# in spinels and Fo in the coexisting olivines within the studied peridotites. The field of oceanic SSZ and passive margin peridotites are from Pearce et al., [27]). OSMA and partial melting trend are from Arai, [35]). 8(b).TiO_2 vs Al_2O_3 variations for cr-spinels of the Hadji-Abad peridotites (fields are from Kamenetsky et al., [47]). (OSMA=Olivine-Spinel Mantle Array)- (OIB= ocean-island basalt)- (LIP= large igneous province)

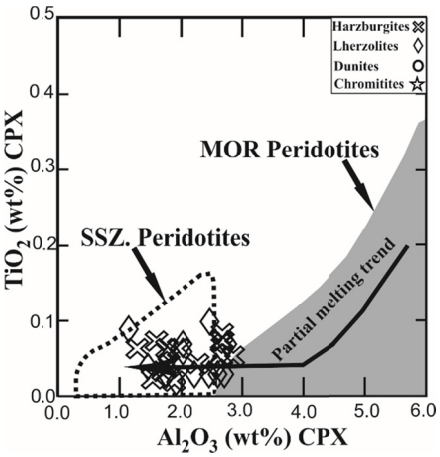

Figure 9. TiO_2 vs Al_2O_3 diagram for clinopyroxenes from the Hadji-Abad peridotites; The range of MOR peridotites and the peridotite range of the suprasubduction zone by Ishii et al,. [48]).

according to Arai [29, 35], the suitable tectonic setting which can have the characteristics of both of these environments is a back arc basin relevant to suprasubduction zone setting.

Conclusion

The petrographical evidences, including different generations of olivine, pyroxene and spinel, as well as the presence of high-temperature deformation textures can indicate the performance of deformation phases in the upper mantle conditions for peridotites of the Hadji-Abad Ultramafic Complex. But low temperature estimates by geo-thermometric studies can be attributed to the subsolidous phase equilibria and emplacement of these rocks in crustal conditions. Different evidences along with mineral chemical data show that the host peridotites from the Hadji-Abad complex have passed a complex history in a suprasubduction zone under high temperature and pressure conditions (the upper mantle) and have undergone some degree of partial melting. The magma involved in the formation of chromitites is similar to those of the boninites which commonly exists in the region above the subduction zones. According to the geological setting of the studied complex and its proximity to the Zagros thrust and its situation in the Neyriz-Kermanshah ophiolites, this complex, like the other complexes in the Esfandagheh region, can be considered as a part of the oceanic lithosphere belonging to Neothetys branches.

Acknowledgment

The authors of this article thank for the financial and logistical support of Shahid Bahonar University of Kerman.

References

1. Rollinson H. Dunites in the mantle section of the Oman ophiolite – The boninite connection, *Lithos,* **334-335**: 1-7 (2019).
2. Uysal I., Kaliwoda M., Karsli O., Tarkian M., Sadiklar M.B., Ottley C.J. Compositional variations as a result of partial melting and malt-peridotite interaction in an Upper mantle section from the Ortaca area, Southwestern Turkey, *Can. Mineral.* **45**: 1471-1493 (2007).
3. Gonzelez-Jimenez J.M., Proenza J.A., Camprubi A., Centeno-Garcia E., Gonzalez-Partida E.,Griffin W.L., O'Reilly S.Y., Pearson N.J. Chromite deposits at Loma Baya: petrogenesis and clues for the origin of the coastal Guerrero Composite Terrane in Mexico*, 11th Biennial meeting SGA, Chile,* (2011).
4. Abdel Halim A. H., Helmy H. M., Elhaddad M.A., El-Mahallawi M. M., Mogessie A. Petrology of a Neoproterozoic mantle peridotite–chromitite association from Abu Dahr area, Eastern Desert, Egypt: Infiltration of a boninitic melt in highly depleted harzburgite, *J. Afr. Earth Sci.* **165:** Article ID 103816 (2020).
5. Su B.X., Chen C., Pang K., Sakyi P. A., U. I., Avci E., Liu X., Zhang P. Melt Penetration in Oceanic Lithosphere: Li Isotope Records from the Pozantı-Karsantı Ophiolite in Southern Turkey, *J. Petrol.* **59**(1): 91–205 (2018).
6. Ghasemi H., Juteau T., Bellon H., Sabzehei M., Witechurch H., Ricou L.M. The mafic–ultramafic complex of Sikhoran (central Iran): a polygenetic ophiolitic complex, *Geoscience*, 334, 431–438 (2002).
7. Ahmadipour H., Sabzehei M., Whitechurch H., Rastad E., and Emami M.H. Soghan complex as an evidence for paleospreading center and mantle diapirism in sananandaj-sirjan zone (South-East Iran), *J.Sci.I.R. of Iran*, **14**(2): 157-172 (2003).
8. Najafzadeh A.R., Ahmadipour H. Using platinum-group elements and Au geochemistry to constrain the genesis of podiformchromitites and associated peridotites from the Soghan mafic–ultramafic complex, Kerman, southeastern Iran, *Ore Geol. Rev.* **60**: 60–75 (2014).
9. Peighambari S., Ahmadipour H., Stosch H.G., Daliran F. Evidence for multi-stage mantle metasomatism at the Dehsheikh peridotite mass if and chromite deposits of the Orzuieh coloured mélange belt, southeastern Iran, *Ore Geol. Rev.* **39**: 245-264 (2011).
10. Mohammadi M. Geochemistry, petrogenesis and economic evaluation of AbBid ultramafic complex, East of Hadji Abad (Hormozgan province). [Ph.D. Thesis]. Shahid Bahonar university of Kerman, (Iran) (2017). (in persian)
11. Ghazi A.M., Pessagno E.A., Hassanipak A.A., Kariminia S.A., Duncan R.A., Babaie H. A. Biostratighraphic zonation and 40Ar/30Ar ages for the Neotethyan Khoy ophiolite of NW Iran, *Palaeogeogr. Palaeoclimatol. Palaeoecol.* **193**: 311-323 (2003).
12. Shafaii Moghadam H., & Stern R. J. Ophiolites of Iran: Keys to understanding the tectonic evolution of SW Asia:(II) Mesozoic ophiolites, *J. Asian Earth Sci.* **100**: 31-

59 (2015).
13. Shafaii Moghadam H., Stern R. J., Chiaradia M. Geochemistry and tectonic evolution of the Late Cretaceous Gogher- Baft ophiolite, central Iran, *Lithos* **168-169**: 33-47 (2013).
14. McCall G.J.H. Explanatory text of the Minab Quadrangle Map; 1:250,000; No. J13, *Geological Survey of Iran, Tehran*, **530** (1985).
15. Shahabpour J. Tectonic evolution of the orogenic belt in the region located between Kerman and neyriz, *J. Asian Earth Sci*. **24**: 405–417 (2005).
16. Sahandi M.R., Azizian H., Nazemzade M., Navazi M., Atapour H. 1/100000 level Orzueiyeh Geological map, *Geological Survey & Mineral exploration of Iran*, Series, No. 7346 (2007).
17. Bonavia F.F., Diella V., and Ferrario A. Precambrian podiformchromitites from KentichaHill, southem Ethiopia, *Econ. Geol.* **88**: 198-202 (1993).
18. Kepezhinskas P. K., Defant M. J., Drummond M .S. Na metasomatism in the island-arc mantle by slab melt-peridotite interaction: evidence from mantle xenoliths in the North Kamchatka arc, *J. Petrol.* **36**, 1505–1527 (1995).
19. Takahashi E. Melting of a dry peridotite KLB I up to 14 GPa: implications on the origin of the peridotitic upper mantle, *J. Geophys. Res.* **91**: 9367-9382 (1986).
20. Ozawa K. Melting and melt segregation in the mantle wedge above a subduction zone: evidence from the chromite-bearing peridotites of the Miyamori Ophiolite Complex, northeastern Japan, *J. Petrol.* **35**: 647 –678 (1994).
21. Page P., Bedard J.H., Schroetter J.M., Tremblay A. Mantle Petrology and Mineralogy of the Thetford Mines ophiolite complex, *Lithos*, **100**: 255-292 (2008).
22. Poldervaart A., and Hess H.H. Pyroxenes in the Crystallization of Basaltic Magma, *J. Geol.* **59**(5): 472-489 (1951).
23. Medaris L.G. High-pressure peridotites in south-western Oregon, *Geol. Soc. Am. Bull.* **83**: 41– 58 (1972).
24. Gaetani G.A., Grove T.L. The influence of water on melting of mantle peridotite, *Contrib. Mineral. Petrol*. **131**: 323-346 (1998).
25. Hirose K., Kawamoto T. Hydrous partial melting of lherzolite at 1GPa: the effect of H_2O on the genesis of basaltic magmas, *Earth. Planet. Sci. Lett.* **133**: 463–473 (1995).
26. Dick H.J.B., Bullen T. Chrome spinel as a petrogenetic indicator in abyssal and alpine-type peridotites and spatially associated lavas, *Contrib. Mineral. Petrol*. **86:** 54–76 (1984).
27. Pearce J.A., Barker P.F., Edwards S.J., Parkinson I.J., Leat P.T. Geochemistry and tectonic significance of peridotites from the South Sandwich arc–basin system, South Atlantic, *Contrib. Mineral. Petrol*. **139:** 36–53 (2000).
28. Zhou M.F. PGE distribution in 27-Ga layered komatiite flows from the Belingwe greenstone belt, Zimbabwe, *Chem. Geol*. **118:** 155-172 (1994).
29. Arai S. Chemistry of Chromian spinel in volcanic rocks as a potential guide to magma chemistry, *Mineral. Mag*. **56:** 173-184 (1992).
30. Nimis P., Taylor W. R. Single clinopyroxene thermometry for garnet peridotites, Calibration and testing of a Cr-in-cpx barometer and enstatite-in-cpx thermometer, *Contrib. Mineral. Petrol.* **139:** 541-554 (2000).
31. Brey G.p., Kohler T. Geothermobarometry in four-phase lherzolites. Part ll: New thermobarometers and practical assessment of existing thermobarometers, *J. Petrol*. **31**: 1353-1378 (1990).
32. Wells P.R.A. Pyroxene thermometry in simple and complex systems, *Contrib. Mineral. Petrol*. **62:** 129-139 (1977).
33. Ionov D. A., Liu Z., Li J., Golovin A.V., Korsakov A.V., Xu Y. The age and origin of cratonic lithospheric mantle: Archean dunites vs. Paleoproterozoic harzburgites from the Udachnaya kimberlite, Siberian craton, *Geochim. Cosmochim. Acta***, 281**: 67-90 (2020).
34. Paulick H., Bach W., Godard M., De Hoog J.C.M., Suhr G., Harvey J. Geochemistry of abyssal peridotites (Mid-Atlantic Ridge, 15°20′N, ODP Leg 209): Implications for fluid/rock interaction in slow spreading environments, *Chem. Geol.* **234:** 179–210 (2006).
35. Arai S. Characterization of spinel peridotites by olivine-spinel compositional relationship: review and interpretation, *Chem. Geol*. **113**: 191–204 (1994).
36. Jiang J.J., Zhu Y., Harzburgite found in the Hegenshan ophiolite, southeastern Central Asian Orogenic Belt: Petrogenesis and geological implications, *Gondwana Res.* **75**: 28-46 (2019)
37. Pearce J.A., Norry M.J. Petrogenetic Implications Of Ti, Zr, Y And Nb Variations In Volcanic Rocks, *Contrib. Mineral. Petrol*. **69:** 33-47 (1979).
38. Parlak O., Hock V., Delaloye M. Suprasubduction zone origin ofthe Pozanti–Karsanti ophiolite (southern Turkey) deduced from wholerockand mineral chemistry of the gabbroic cumulates, In: Tectonicsand Magmatism in Turkey and the Surrounding Area, Bozkurt, E.,Winchester, J.A., Piper, J.D.A. (eds.), *Geol. Soc. Spec. Publ.* **173**: 219–234 (2002).
39. Vergili O., Parlak O. Geochemistry and tectonic setting of metamorphic sole rocks and mafic dikes from the Pınarbaşı (Kayseri) ophiolite, Central Anatolia, *Ofioliti,* **30**: 37–52 (2005).
40. Rızaoğlu T., Parlak O., Hock V., İşler F. Nature and significance of Late Cretaceous ophiolitic rocks ands its relation to the Baskil granitoid in Elazığ region, SE Turkey. In: Robertson, A.H.F. & Mountrakis, D. (eds), Tectonic Development of the Eastern Mediterranean, *Geol. Soc. Spec. Publ.* **260:** 327–350 (2006).
41. Dilek Y. and Thy P. Island arc tholeiite to boninitic melt evolution of the Cretaceous Kızıldağ (Turkey) ophiolite: model for multistage early arc–forearc magmatism in Tethyan subduction factories, *Lithos* **113:** 68–87 (2009).
42. Stöcklin J. Structural correlation of the Alpine range between Iran and Central Asia. *Memoire Hors-Serie no.8, de la Societe Geologique de la France,* **8:** 333-353 (1977).
43. Rajabzadeh M.A., Dehkordi T.N. Investigation on mantle peridotites from Neyriz ophiolite, south of Iran: geodynamic signals, *Arab. J. Geosci.* **6**(11): 4445-4461 (2013).
44. Shafaii Moghadam H., Whitechurch H., Rahgoshay M. and Monsef I. Significance of Nain - Baft ophiolitic belt (Iran): Short - lived, transtensional Cretaceous back-arc oceanic basins over the Tethyan subduction zone, *C. R. Geosci*.

341: 1016-1028 (2009).
45. Ahmadipour A., Shahabpour J. Petrological evoloution of the upper mantle beneath the southern Sanandaj-Sirjan zone: Evidence from Kushah peridotite massif, Southeast Iran, *J.Sci.I.R. of Iran*, **25**(1), 35-49 (2014).
46. Mercier J.C.C., Nicolas A. Textures and fabrics of upper mantle peridotites as illustrated by xenoliths from basalts, *J. Petrol.* **16**: 454–487 (1975).
47. Kamenetsky V.S, Crawford A.J, Meffre S. Factors controlling chemistry of magmatic spinel: an empirical study of associated olivine, Cr-spinel and melt inclusions from primitive rocks, *J. Petrol*. **42**: 655–671 (2001).
48. Ishii T.**,** Robinson P**.**T**.,** Maekawa H., Fiske R**.** Petrological studies of peridotites from diapiric serpentinite seamounts in the Izu-Ogasawara-Mariana Forearc, Leg 125. In: Fryer, P; Pearce, JA; Stokking, LB; et al. (eds.), *Proc. ODP*, *Sci. Results*, **125**: 445-485 (1992).